The Journal of Chemical Physics

A noniterative perturbative triples correction for the spin-flipping and spin-conserving equation-of-motion coupled-cluster methods with single and double substitutions

Cite as: J. Chem. Phys. **129**, 194105 (2008); https://doi.org/10.1063/1.3013087
Submitted: 25 August 2008 . Accepted: 13 October 2008 . Published Online: 18 November 2008

Prashant U. Manohar, and Anna I. Krylov

View Online Export Citation

ARTICLES YOU MAY BE INTERESTED IN

The equation of motion coupled-cluster method. A systematic biorthogonal approach to molecular excitation energies, transition probabilities, and excited state properties
The Journal of Chemical Physics **98**, 7029 (1993); https://doi.org/10.1063/1.464746

Gaussian basis sets for use in correlated molecular calculations. I. The atoms boron through neon and hydrogen
The Journal of Chemical Physics **90**, 1007 (1989); https://doi.org/10.1063/1.456153

Excited states from modified coupled cluster methods: Are they any better than EOM CCSD?
The Journal of Chemical Physics **146**, 144104 (2017); https://doi.org/10.1063/1.4979078

AIP Publishing

© 2008 American Institute of Physics.

A noniterative perturbative triples correction for the spin-flipping and spin-conserving equation-of-motion coupled-cluster methods with single and double substitutions

Prashant U. Manohar and Anna I. Krylov[a)]
Department of Chemistry, University of Southern California, Los Angeles, California 90089-0482, USA

(Received 25 August 2008; accepted 13 October 2008; published online 18 November 2008)

A noniterative N^7 triples correction for the equation-of-motion coupled-cluster method with single and double substitutions (CCSD) is presented. The correction is derived by second-order perturbation treatment of the similarity-transformed CCSD Hamiltonian. The spin-conserving variant of the correction is identical to the triples correction of Piecuch and co-workers [Mol. Phys. **104**, 2149 (2006)] derived within method-of-moments framework and is not size intensive. The spin-flip variant of the correction is size intensive. The performance of the correction is demonstrated by calculations of electronic excitation energies in methylene, nitrenium ion, cyclobutadiene, *ortho*-, *meta*-, and *para*-benzynes, 1,2,3-tridehydrobenzene, as well as C–C bond breaking in ethane. In all cases except cyclobutadiene, the absolute values of the correction for energy differences were 0.1 eV or less. In cyclobutadiene, the absolute values of the correction were as large as 0.4 eV. In most cases, the correction reduced the errors against the benchmark values by about a factor of 2–3, the absolute errors being less than 0.04 eV. © *2008 American Institute of Physics*. [DOI: 10.1063/1.3013087]

I. INTRODUCTION

The equation-of-motion coupled-cluster (EOM-CC) family of methods[1–9] allows one to compute a variety of electronically excited and open-shell wave functions in an efficient and robust single-reference procedure.[10–16] Similar (or even identical) equations can be derived within linear response CC[17–20] or symmetry-adapted cluster configuration interaction formalisms.[21,22] EOM-CC with single and double substitutions for excitation energies (EEs), EOM-EE-CCSD,[4,18,23] describes electronic states with predominantly singly excited character with accuracy of 0.1–0.3 eV.[24] Even smaller errors have been observed for the spin-flip (SF) variant, EOM-SF-CCSD.[5,25]

Unfortunately, the EOM-CCSD performance deteriorates for electronic states with large contributions of double excitations as, for example, dark states of polyenes, or some valence states of radicals. Moreover, the EOM-CCSD accuracy degrades when the reference wave function is spin contaminated or is poorly described by a single determinant. Inclusion of triple excitations rectifies these problems, which originate in incomplete treatment of nondynamical correlation, and also improves accuracy for well-behaved excited states by more complete accounting of dynamical correlation. For example, the error bars of EOM-CCSDT and its approximate variant, EOM(2,3), are 0.1 eV for the states with large doubly excited character and 0.01 eV for singly excited states.[24,26,27] Equilibrium structures and vibrational frequencies of electronically excited states are also greatly improved upon explicit inclusion of triple excitations.[28,29]

Unfortunately, the resulting N^8 scaling limits the applicability of models with explicit triples, and a number of N^7 approximations to full EOM-CCSDT[30–33] were reported. Watts and Bartlett[34] implemented an approximate EOM-CCSDT model, in which only two-body elements in the triples blocks of the similarity-transformed Hamiltonian were included, iterative EOM-CCSDT-1 and EOM-CCSDT-3 models and their noniterative counterparts EOM-CCSD(T) and EOM-CCSD($\tilde{\mathrm{T}}$).[35–37] The iterative CC3 and the noniterative CCSDR(3) models were introduced by Koch *et al.*,[38–40] and recently extended to open-shell references by Smith *et al.*[41] Kowalski and Piecuch[42–44] introduced several models for triples corrections derived within method-of-moments framework: See, for example, their recent formulation of renormalized CC methods.[45–47]

Some of these approaches, e.g., CC3 and CR-CCSD(T)$_L$ [completely renormalized CCSD(T) using left EOM eigenvectors], also produce accurate and size-extensive triples corrections for the reference CCSD wave functions. CR-CCSD(T)$_L$ and earlier perturbative corrections utilizing left coupled-cluster eigenvectors,[48–53] i.e., a-CCSD(T), Λ-CCSD(T), and CCSD(2), have been shown to be more robust than the popular CCSD(T) method.[54,55]

This work introduces a noniterative N^7 triples correction for the EOM-CCSD energies derived by second-order perturbation treatment of the similarity-transformed CCSD Hamiltonian. The implementation avoids storing of six-index tensors. Our formalism (and the resulting correction) is very similar to the approach of Stanton and Gauss,[56] who were the first to use this type of perturbation theory (in the context of triples correction to EOM-CCSD) and employed Rayleigh–Schrödinger perturbation theory to derive triples correction for the EOM-CCSD for ionization potentials

a)Electronic mail: krylov@usc.edu.

 © 2008 American Institute of Physics

(EOM-IP-CCSD) method, and to a more recent work of Hirata *et al.*[57] The focus of this work is on the SF variant of EOM-CCSD. For CCSD and EOM-EE-CCSD, the correction is identical to the CR-CCSD(T)$_L$ method of Piecuch and co-workers[45,47] The SF correction is size intensive, whereas the EE counterpart is not.

II. THEORY

We begin by considering CCSD similarity-transformed Hamiltonian $\bar{H}$,

$$\bar{H} = e^{-(T_1+T_2)} H e^{T_1+T_2}, \tag{1}$$

where T_1 and T_2 are operators generating all single and double excited determinants from reference Φ_0 satisfying the CC equations for the reference state. Note that regardless of the choice of T, the exact ground and excited state energies can be obtained by diagonalizing $\bar{H}$ in the full configuration space $\{\Phi_0, \Phi_1, \Phi_2, \ldots, \Phi_N\} \equiv \{\mathrm{O,S,D,}\ldots\mathrm{N}\}$, where Φ_0 and Φ_μ denote the reference and μ-tuply excited Slater determinants, respectively.

With T_1 and T_2 satisfying the CC equations for the reference state, the diagonalization of $\bar{H}$ in the {O,S,D} space yields the reference CCSD and EOM-CCSD excitation energies,

$$\bar{H} R^k = E_k R^k, \tag{2}$$

$$R^0 = 1, \tag{3}$$

$$R^{k\neq 0} = R_0^k + R_1^k + R_2^k, \tag{4}$$

where the operators R_μ^k generate all possible μ-tuply excited determinants from the reference. Because $\bar{H}$ is non-Hermitian, its left and right eigenstates are not complex conjugates of each other but can be chosen to form a biorthonormal set,

$$\langle \Phi_0 L^k | R^l \Phi_0 \rangle = \delta_{kl}, \tag{5}$$

$$L^k = L_1^k + L_2^k. \tag{6}$$

By splitting $\bar{H}$ into a zero-order part H_0 (to be specified later) and the perturbation $V \equiv \bar{H} - H_0$ and adapting second-order perturbation theory to a non-Hermitian Hamiltonian, we arrive to the following general expressions:

$$H_0 |\Psi_k^{(0)}\rangle = E_k^{(0)} |\Psi_k^{(0)}\rangle, \tag{7}$$

$$\langle \tilde{\Psi}_k^{(0)} | H_0 = E_k^{(0)} \langle \tilde{\Psi}_k^{(0)} |, \tag{8}$$

$$E_k^{(1)} = \langle \tilde{\Psi}_k^{(0)} | V | \Psi_k^{(0)} \rangle, \tag{9}$$

$$(H_0 - E_k^{(0)}) |\Psi_k^{(1)}\rangle = -(V - E_k^{(1)}) |\Psi_k^{(0)}\rangle, \tag{10}$$

$$E_k^{(2)} = \langle \tilde{\Psi}_k^{(0)} | V | \Psi_k^{(1)} \rangle, \tag{11}$$

where left $\langle \tilde{\Psi}_k |$ and right $|\Psi_l\rangle$ eigenfunctions satisfy the following biorthonormality conditions:

$$\langle \tilde{\Psi}_k^{(0)} | \tilde{\Psi}_l^{(0)} \rangle = \delta_{kl}, \tag{12}$$

$$\langle \tilde{\Psi}_k^{(0)} | \tilde{\Psi}_k^{(1)} \rangle = 0. \tag{13}$$

We define H_0 such that $E_k^{(0)}$ and $\Psi_k^{(0)}$ correspond to the CCSD/EOM-CCSD energies and wave functions. Thus, the matrix of H_0 is block diagonal: In the {O,S,D} block, it is simply the matrix of $\bar{H}$ in the basis of the reference, singly, and doubly excited determinants, and the rest of it is zero except for the diagonal terms, e.g.,

$$\langle T | H_0 | T \rangle = \langle \Phi_{ijk}^{abc} | \bar{H} | \Phi_{ijk}^{abc} \rangle. \tag{14}$$

Thus, our choice of H_0 is almost identical to that of Stanton and Gauss[56] and Hirata *et al.*,[57] who applied Rayleigh–Schrödinger perturbation theory (PT) to the CC and EOM-CC wave functions. In the {O,S,D} block, all three H_0 are identical. For the {T,Q,…,} part of H_0, we choose to take the exact diagonal of the CCSD $\bar{H}$ as given by Eq. (14), whereas Hirata *et al.* used the bare Möller–Plesset orbital energy differences, as did Stanton and Gauss.[56] We implemented both variants, and our numerical examples demonstrate the difference between the two choices of the *TT* part of H_0. Similar derivation of the EOM-CCSD(T) and EOM-CCSD($\tilde{T}$) corrections[36,37] has been presented by Watts *et al.*[58] The important difference between the derivations in Refs. 56 and 58 and the one employed here (and in Ref. 57) is that we treat the CCSD $\bar{H}$ as the Hamiltonian of the Rayleigh–Schrödinger PT and define the perturbation V as the difference between the CCSD $\bar{H}$ in the {O,S,D,T} space and H_0, whereas Refs. 56 and 58 choose their Hamiltonian (and, consequently, perturbation V) slightly differently and perform additional perturbative expansions by orders of T.

As follows from the above choice of H_0 and V, the matrix of the perturbation V is zero in the {O,S,D} block and on the diagonal. Note that the off-diagonal blocks of V are the moments (more often called projections) of the CC equations,

$$\langle T | V | \Phi_0 \rangle = \langle \Phi_{ijk}^{abc} | \bar{H} | \Phi_0 \rangle, \tag{15}$$

$$\langle Q | V | \Phi_0 \rangle = \langle \Phi_{ijkl}^{abcd} | \bar{H} | \Phi_0 \rangle,$$

$$\ldots. \tag{16}$$

By virtue of a block-diagonal form of H_0, the first-order energy correction is zero and the first-order correction to the wave functions $\Psi_k^{(1)}$ does not include reference, singly, or doubly excited determinants. The amplitudes of triple and quadruple excitations are defined by Eq. (10). Neglecting quadruple excitations, we arrive to

$$\Psi_m^{(1)} = \frac{1}{(3!)^2} \sum_{ijkabc} R_{ijk}^{abc} \Phi_{ijk}^{abc}, \tag{17}$$

$$R_{ijk}^{abc} = -\frac{\sigma_{ijk}^{abc}}{D_{ijkabc}^m}, \tag{18}$$

TABLE I. R-independent intermediates used in the (dT) and (fT) energy expressions.

$$F_{ia} = f_{ia} + \sum_{jb} t_j^b \langle ij||ab\rangle$$

$$F_{ij} = f_{ij} + \sum_a t_i^a f_{ja} + \sum_{ka} t_k^a \langle jk||ia\rangle + \sum_{kab} t_i^a t_k^b \langle jk||ab\rangle + \frac{1}{2}\sum_{kbc} t_{ik}^{bc} \langle jk||bc\rangle$$

$$F_{ab} = f_{ab} - \sum_i t_i^a f_{ib} - \sum_{ic} t_i^c \langle ia||bc\rangle + \sum_{ijc} t_i^c t_j^a \langle ij||bc\rangle - \frac{1}{2}\sum_{jkc} t_{jk}^{ac} \langle jk||bc\rangle$$

$$I_{iajb}^1 = \langle ia||jb\rangle - \sum_k t_k^b \langle jk||ia\rangle - \sum_c t_i^c \langle jb||ac\rangle + \sum_{kc} t_i^c t_k^b \langle jk||ac\rangle - \sum_{kc} t_{ik}^{bc} \langle jk||ac\rangle$$

$$I_{ijka}^2 = -\langle ij||ka\rangle + 2\sum_l t_l^a I_{ijkl}^4 + P(ij)\sum_b \left(t_i^b\left(\langle jb||ka\rangle - \sum_{lc} t_{jl}^{ac}\langle kl||bc\rangle\right)\right) - \sum_{bc} t_i^b t_j^c \langle ka||bc\rangle - \sum_{lbc} t_l^b t_{ij}^{ac} \langle kl||bc\rangle$$
$$+ \sum_c t_{ij}^{bc} f_{kc} - \frac{1}{2}\sum_{cd} t_{ij}^{cd} \langle kb||cd\rangle + P(ij)\sum_{lc} t_{il}^{bc} \langle jc||kl\rangle$$

$$I_{icab}^3 = -\langle ic||ab\rangle + 2\sum_d t_i^d I_{bcad}^5 + P(bc)\sum_j \left(t_j^b\left(\langle ia||jc\rangle - \sum_{kd} t_{ik}^{cd}\langle jk||ad\rangle\right)\right) - \sum_{jk} t_j^b t_k^c \langle jk||ia\rangle - \sum_{jkd} t_j^d t_{ik}^{bc} \langle jk||ad\rangle$$
$$+ \sum_k t_{ik}^{ab} f_{kc} - \frac{1}{2}\sum_{kl} t_{kl}^{ab} \langle ic||kl\rangle + P(ab)\sum_{kd} t_{ik}^{ad} \langle kb||cd\rangle$$

$$I_{ijkl}^4 = \frac{1}{2}\langle ij||kl\rangle - \frac{1}{2}P(ij)\sum_a t_i^a \langle kl||ja\rangle + \frac{1}{2}\sum_{ab} t_i^a t_j^b \langle kl||ab\rangle + \frac{1}{4}\sum_{cd} t_{ij}^{cd} \langle kl||cd\rangle$$

$$I_{abcd}^5 = \frac{1}{2}\langle ab||cd\rangle - \frac{1}{2}\sum_i \left(t_i^a \langle ib||cd\rangle - t_i^b \langle ia||cd\rangle\right) + \frac{1}{2}\sum_{ij} t_i^a t_j^b \langle ij||cd\rangle + \frac{1}{4}\sum_{kl} t_{kl}^{ab} \langle kl||cd\rangle$$

$$I_{ijka}^6 = \langle ij||ka\rangle - \sum_c t_k^c \langle ij||ac\rangle$$

$$I_{iabc}^7 = \langle ia||bc\rangle - \sum_j t_j^a \langle ij||bc\rangle$$

$$\sigma_{ijk}^{abc} = [\langle \Phi_{ijk}^{abc}|\bar{H}|\Phi_0\rangle \cdot R_0 + \langle \Phi_{ijk}^{abc}|\bar{H}|R_1\Phi_0\rangle + \langle \Phi_{ijk}^{abc}|\bar{H}|R_2\Phi_0\rangle], \tag{19}$$

$$D_{ijkabc}^m = \langle \Phi_{ijk}^{abc}|\bar{H}|\Phi_{ijk}^{abc}\rangle - E_m^{(0)}. \tag{20}$$

Note that σ_{ijk}^{abc} are the same as the right σ vectors for the Davidson procedure in EOM(2,3) minus the contributions from the triply excited EOM(2,3) amplitudes.[27] By combining the above with Eq. (11), the second-order energy correction assumes the following form:

$$E_m^{(2)} = -\frac{1}{(3!)^2}\sum_{ijkabc} \frac{\tilde{\sigma}_{ijk}^{abc}\sigma_{ijk}^{abc}}{D_{ijkabc}^m}$$
$$= -\frac{1}{(3!)^2}\sum_{ijkabc} \frac{\langle \Phi_0 L^m|\bar{H}|\Phi_{ijk}^{abc}\rangle\langle \Phi_{ijk}^{abc}|\bar{H}|R^m\Phi_0\rangle}{D_{ijkabc}^m}, \tag{21}$$

where L^k and R^k are the left and right EOM-CCSD eigenvectors for state $k \neq 0$, respectively. For the reference state, $R^0 \equiv 1$ and $L^0 \equiv \Lambda_1 + \Lambda_2$, and the energy correction is identical to the CR-CCSD(T)$_L$ expression.[46]

The $\tilde{\sigma}$ vector from Eq. (21) is

$$\tilde{\sigma}_{ijk}^{abc} = \langle \Phi_0 L_1|\bar{H}|\Phi_{ijk}^{abc}\rangle + \langle \Phi_0 L_2|\bar{H}|\Phi_{ijk}^{abc}\rangle. \tag{22}$$

Using the intermediates defined in Refs. 5, 59, and 60, the programmable expressions for $\tilde{\sigma}$ become

$$\langle \Phi_0 L_1|\bar{H}|\Phi_{ijk}^{abc}\rangle = P(i|jk)P(a|bc)l_i^a\langle jk||bc\rangle, \tag{23}$$

$$\langle \Phi_0 L_2|\bar{H}|\Phi_{ijk}^{abc}\rangle = P(i|jk)P(a|bc)l_{jk}^{bc}F_{ia} - P(i|jk)P(ab|c)\sum_l l_{il}^{ab} I_{jklc}^6 + P(ij|k)P(a|bc)\sum_d l_{ij}^{ad} I_{kdcb}^7. \tag{24}$$

The σ-vector from Eq. (19) can be retrieved from Ref. 27 and consists of the following blocks:

$$\langle \Phi_{ijk}^{abc}|\bar{H}|R_0\Phi_0\rangle = R_0 \cdot \left[P(a|bc)P(ij|k)\sum_l t_{lk}^{bc}\left(-I_{ijla}^2 + \sum_d t_{ij}^{ad} F_{ld}\right) + \sum_d t_{ij}^{ad} I_{kdbc}^3\right], \tag{25}$$

$$\langle \Phi_{ijk}^{abc}|\bar{H}|R_1\Phi_0\rangle = P(a|bc)P(ij|k)\left(\sum_l t_{kl}^{bc} H_{ijla}^2 + \sum_d t_{ij}^{ad} H_{kdbc}^3\right), \tag{26}$$

$$\langle \Phi_{ijk}^{abc}|\bar{H}|R_2\Phi_0\rangle = P(a|bc)P(ij|k)\left[\sum_d (r_{ij}^{ad} I_{kdbc}^3 + t_{ij}^{ad} H_{kdbc}^5) + \sum_l (r_{kl}^{bc} I_{ijla}^2 + t_{kl}^{bc} H_{ijla}^4)\right]. \tag{27}$$

The intermediates in the above equations are defined in Refs. 5, 27, 59, and 60, and are summarized in Tables I and II.

The expression for the diagonal D_{ijkabc}^m from Eq. (21) is

TABLE II. H-intermediates used in the (dT) and (fT) energy expressions.

$$H^2_{jklc} = 2\sum_m r^c_m I^4_{jklm} + P(jk)\sum_d r^d_j I^1_{kdlc}$$

$$H^3_{kdbc} = -2\sum_e r^e_k I^5_{bced} + P(bc)\sum_l r^b_l I^1_{kdlc} + \sum_l H^1_{ld} t^{bc}_{kl}$$

$$H^4_{jklc} = -1/2\sum_{ab} r^{ab}_{jk} I^7_{lcab} + P(jk)\sum_{ai} r^{ca}_{ji} I^6_{lika}$$

$$H^5_{kdbc} = -1/2\sum_{ij} r^{bc}_{ij} I^6_{ijkd} - P(bc)\sum_{ia} r^{ba}_{ki} I^7_{icad}$$

$$\begin{aligned} D^m_{ijkabc} &= \langle \Phi^{abc}_{ijk} | \bar{H} | \Phi^{abc}_{ijk} \rangle - (E_{CC} + \omega_m) \\ &= -P(ijk)F_{ii} + P(abc)F_{aa} + 2 \cdot P(ij|k)I^4_{ijij} \\ &\quad + 2 \cdot P(ab|c)I^5_{abab} - P(i|jk)P(a|bc)I^1_{iaia} \\ &\quad - P(ij|k)P(a|bc)\left[\sum_d t^{ad}_{ij}\langle ij||ad\rangle \right. \\ &\quad \left. + \sum_l t^{ab}_{kl}\langle kl||ab\rangle\right] - \omega_m, \end{aligned} \tag{28}$$

where E_{CC} and ω_m are the total ground state CCSD and the EOM excitation energies, respectively.

We implemented two variants of the triples correction defined by Eq. (21): (i) Using the full $\bar{H}$ diagonal as defined by Eq. (28); and (ii) using the canonical (or semicanonical) Hartree–Fock orbital energy differences, i.e., $-P(ijk)\epsilon_i + P(abc)\epsilon_a$. They will be referred to as EOM-CCSD(dT) and EOM-CCSD(fT), respectively (i.e., diagonal and Fock triples). For the non-SF calculations, the former is identical to the CR-CCSD(T)$_L$ method,[45,46] and the latter to the CR-CCSD(T)$_2$ approximation. Moreover, the EOM-CCSD(fT) correction is identical to the triples-only part of EOM-CC(2)PT(2) from Ref. 57. Computational costs of (dT) and (fT) are, of course, very similar.

It should be noted that EOM-CCSD(dT) is not fully orbitally invariant in the case of degenerate virtual orbitals, whereas EOM-CCSD(fT) is (assuming canonical orbitals are used). A simple solution to this problem, diagonalizing $\bar{H}$ blocks in the subspace of degenerate orbitals, has been suggested by Piecuch and Włoch.[46] In the case of symmetry-imposed degeneracies (i.e., non-Abelian point groups), one can request that the orbitals belong to irreducible representations of a largest Abelian subgroup, which is a common practice in electronic structure codes. Orbital invariance (or lack of thereof) of different perturbative approaches has recently been discussed by Taube and Bartlett.[52]

As follows from our choice of H_0+V, (dT) can also be described as a perturbative approximation to the EOM-CC(2,3) method.[27] Similarly to EOM-CC(2,3), the EE variant of the correction for the target EOM states ($m>0$) is not size intensive, except for the states of the symmetry different from that of the reference; however, the EOM-SF-CCSD(dT) and EOM-SF-CCSD(fT) energies and energy differences computed as $E_k - E_i$, $i \neq 0$, from Eq. (21) are size intensive,[61] just as those of EOM-SF-CCSD (Ref. 14) or EOM-SF(2,3).[27] This difference between the size intensivity of the EOM-EE and EOM-SF variants of the correction, which can be traced to nonzero R_0 in the former, is demonstrated by a numerical example below.

The (dT) correction for the reference $m=0$ state is size extensive and is identical to CR-CCSD(T)$_L$.[45] Using perturbative treatment of the similarity-transformed CCSD $\bar{H}$ to derive triples corrections to the ground state CCSD energies has been discussed in Ref. 56 (see footnote 19), and exploited in several approaches utilizing the left coupled-cluster eigenfunction.[48–53] For the detailed comparative analysis of different triples corrections to the CCSD energies, see the recent paper of Taube and Bartlett.[52]

The EOM-SF/EE-CCSD(fT) and EOM-SF/EE-CCSD(dT) energy expressions using the above equations are implemented within the Q-CHEM electronic structure package.[62] Further details of implementation are given in the Appendix.

III. RESULTS AND DISCUSSION

EOM-SF-CCSD(fT) and EOM-SF-CCSD(dT) are benchmarked using several prototypical diradicals, e.g., methylene, nitrenium ion, and the o-, m-, and p-benzyne diradicals, as well as the 1,2,3 tri-dehydrobenzene triradical (TDB). We also present results for the low-lying electronic states of cyclobutadiene, which has considerable diradical character. We use this example to compare the performance of the SF methods against the non-SF counterparts. Moreover, we present potential energy scans along CC bond-breaking coordinate in ethane.[63] Size extensivity of the method is demonstrated by calculating excitation energies in methylene and methylene-neon.

A. Computational details

Methylene and nitrenium calculations are performed using the same equilibrium geometries as in Ref. 25, i.e., FCI/TZ2P and CISD/TZ2P(f,d) optimized structures, respectively.[64,65] For methylene, we employed the TZ2P basis from Ref. 64, and for nitrenium we used TZ2Pf basis set derived from the TZ basis set[66,67] by augmenting it by two sets of polarization functions ($\alpha_p=1.50$ and 0.375 for hydrogen and $\alpha_d=1.60$ and 0.40 for nitrogen) and by higher angular momentum functions ($\alpha_d=1.00$ for hydrogen and $\alpha_f=1.00$ for nitrogen). The size-extensivity calculations were performed using the above geometry and basis for methylene and the cc-pVTZ[68] basis for neon. The C–Ne distance is 100 Å with Ne on the C_{2v} axis of methylene (on the concave side).

The unrestricted Hartree–Fock (UHF) triplet references were used in the CH_2, NH_2^+, CH_2–Ne, and ethane calculations. For benzynes, TDB, and cyclobutadiene we employed restricted open-shell Hartree–Fock (ROHF) high-spin references to mitigate the effects of spin contamination. For cyclobutadiene, we present both the UHF and ROHF based results.

The calculations for cyclobutadiene were performed using equilibrium geometries of the ground $X\ ^1A_g$ and $1\ ^3A_{2g}$ states optimized at the CCSD(T)/cc-pVTZ level of theory[54] from Ref. 5. The cc-pVTZ basis[68] was employed during the calculations.

TABLE III. Total energies of ground state ($\tilde{X}\,^3B_1$) (hartree) and vertical excitation energies (eV) of CH_2 and CH_2–Ne.

Method	$\tilde{X}\,^3B_1$	$\tilde{a}\,^1A_1$	$\tilde{b}\,^1B_1$	$\tilde{c}\,^1A_1$
CH_2				
EOM-SF-CCSD	−39.080 46	0.991	1.587	3.325
EOM-SF-CCSD(fT)	−39.081 84	0.977	1.575	3.297
EOM-SF-CCSD(dT)	−39.082 17	0.974	1.571	3.287
CH_2–Ne				
EOM-SF-CCSD	−167.891 27	0.991	1.587	3.325
EOM-SF-CCSD(fT)	−167.892 66	0.977	1.575	3.297
EOM-SF-CCSD(dT)	−167.892 98	0.974	1.571	3.287

The calculations of benzynes were performed using cc-pVTZ basis and the geometries as in Ref. 69, i.e., optimized at the SF-TDDFT/6-31G* level using 50/50 functional.[70]

The TDB calculations were performed with the 6-31G* and cc-pVTZ bases, at the B3LYP/cc-pVTZ optimized equilibrium geometries of the $^2B_2$ and $^2A_1$ states.[71]

The ethane calculations employed the aug-cc-pVTZ basis set. The methyl groups were frozen at the planar staggered configuration as in Ref. 63.

All electrons were correlated in the methylene, nitrenium, cyclobutadiene, and TDB calculations. In benzynes, six core orbitals and five highest virtual orbitals were frozen. Two core orbitals and two virtual orbitals were frozen in the ethane calculations.

Pure angular momentum polarization functions were employed in all the calculations except for the 6-31G* calculations of TDB.

All the calculations were performed using Q-CHEM electronic structure package[62] Relevant molecular structures and total energies are available as EPAPS.[72]

B. Size extensivity of EOM-CCSD(fT) and EOM-CCSD(dT)

Both EOM-EE-CCSD and EOM-SF-CCSD are size intensive,[61] however, the (dT) and (fT) corrections are only size intensive for EOM-SF. This section presents a numerical example demonstrating this difference.

Table III presents the total energy of the $\tilde{X}\,^3B_1$ ground state and vertical excitation energies for methylene and methylene-neon.

TABLE IV. Total energies (hartree) of the (a^1A_1) state and vertical excitation energies (eV) for CH_2 and CH_2–Ne.

Method	$a\,^1A_1$	$\tilde{c}\,^1A_1$	$\tilde{b}\,^1B_1$	$^3B_1$
CH_2				
EOM-EE-CCSD	−39.041 97	3.767	0.537	−1.053
EOM-EE-CCSD(fT)	−39.046 33	2.739	0.593	−0.977
EOM-EE-CCSD(dT)	−39.047 33	2.632	0.606	−0.956
CH_2–Ne				
EOM-EE-CCSD	−167.852 79	3.767	0.537	−1.053
EOM-EE-CCSD(fT)	−167.861 18	2.848	0.703	−0.867
EOM-EE-CCSD(dT)	−167.862 76	2.488	0.732	−0.831

TABLE V. Total energies of ground state ($\tilde{X}\,^3B_1$) and adiabatic excitation energies (eV) of CH_2.

Method	$\tilde{X}\,^3B_1$	$\tilde{a}\,^1A_1$	$\tilde{b}\,^1B_1$	$\tilde{c}\,^1A_1$
FCI	−39.066 74	0.483	1.542	2.674
SF-CIS(D)	−39.055 86	0.613	1.646	2.953
EOM-SF-CCSD	−39.080 46	0.517	1.565	2.718
EOM-SF-CCSD(fT)	−39.081 84	0.500	1.552	2.688
EOM-SF-CCSD(dT)	−39.082 17	0.496	1.548	2.678

As in the case of EOM-SF-CCSD, the EOM-SF-CCSD(fT) and EOM-SF-CCSD(dT) excitation energies are not affected by the presence of neon 100 Å away. The difference between the total ground state energies of CH_2 and CH_2–Ne is 128.81081 hartree, which is the CCSD/cc-pVTZ ground state energy of neon.

Table IV presents the results of EOM-EE calculations using closed-shell singlet reference. The behavior of EOM-EE-CCSD(fT) and EOM-EE-CCSD(dT) is different. Whereas the energy of the reference $^1A_1$ state of the combined system is the sum of the respective total energies of CH_2 and Ne, the excitation energies with respect to the singlet state are different in CH_2–Ne and CH_2, i.e., the excitation energies in the combined system are 0.13–0.14 eV lower than in bare CH_2. Note that the energy differences between the $^3B_1$ and $^1B_1$ states are not affected by Ne.

C. Methylene and nitrenium ion

The adiabatic excitation energies of the three diradical states of CH_2 are summarized in Table V. The FCI and SF-CIS(D) data are from Refs. 64 and 25, respectively. The differences with respect to FCI are presented in Fig. 1. The triples correction results in a small decrease in the excitation energies, the absolute value of (dT) correction being 0.002–

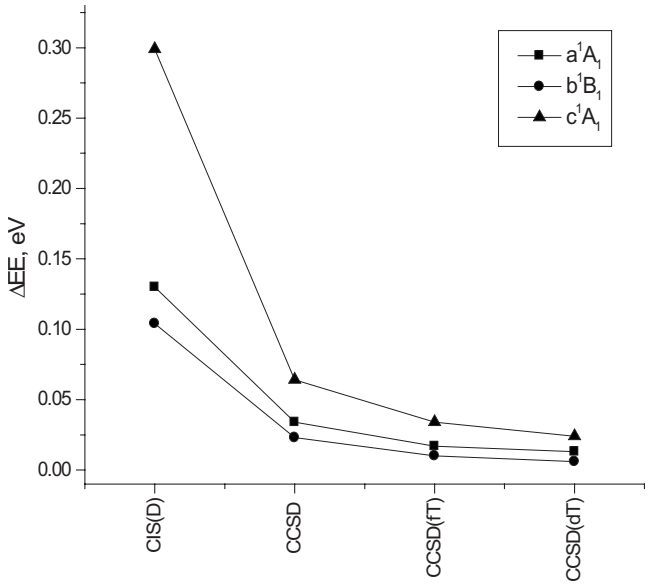

FIG. 1. Differences against FCI in excitation energies of methylene, TZ2P basis.

TABLE VI. Total energies of ground state ($\tilde{X}\ ^3B_1$) and adiabatic excitation energies (eV) of NH_2^+.

Method	$\tilde{X}\ ^3B_1$	$\tilde{a}\ ^1A_1$	$\tilde{b}\ ^1B_1$	$\tilde{c}\ ^1A_1$
SF-CIS	−55.227 31	1.673	2.151	4.375
SF-CIS(D)	−55.375 45	1.342	1.959	3.635
EOM-SF-CCSD	−55.402 54	1.306	1.918	3.420
EOM-SF-CCSD(fT)	−55.404 19	1.292	1.905	3.391
EOM-SF-CCSD(dT)	−55.404 43	1.289	1.902	3.382
CASSCF SOCI[a]	−55.388 37	1.281	1.935	3.380
Expt.[b]		1.306 ± 0.010		

[a]From Ref. 65.
[b]From Ref. 75.

0.003 eV. As expected, the errors against FCI decrease in the CIS(D) → CCSD → CCSD(fT) → CCSD(dT) series. The absolute errors in the EOM-SF-CCSD excitation energies decrease by a factor of 3–10 upon inclusion of triples. The EOM-SF-CCSD(dT) excitation energies are within 0.004–0.013 eV from FCI.

NH_2^+, which is isoelectronic and isovalent to CH_2, exhibits similar trends. The results, as well as the benchmark SOCI values,[65] are summarized in Table VI and visualized in Fig. 2. The absolute values of the correction are 0.02–0.05 eV. Whereas the errors in CCSD excitations for the A_1 states are 0.025–0.04 eV, the (fT) and (dT) corrections reduce them to 0.01 eV and below. For the $^1B_1$ state, the CCSD-CCSD(fT)/(dT) errors are about 0.03 eV slightly exceeding the EOM-SF-CCSD value.

D. Cyclobutadiene

The diradical character of cyclobutadiene depends on the geometry. At the equilibrium (D_{2h}) geometry of the ground state, the highest occupied molecular orbital and lowest unoccupied molecular orbital are nondegenerate, and the diradical character is relatively weak, however, at the equilibrium geometry of the triplet state, the orbitals are exactly degenerate and single-reference methods fail. Note that even at the D_{4h} geometry, the triplet state is above the singlet, thus violating Hund's rule of maximum multiplicity. Tables VII and VIII summarize the calculations at the $X\ ^1A_g$ (ground) state and $^3A_{2g}$ state equilibrium geometries.

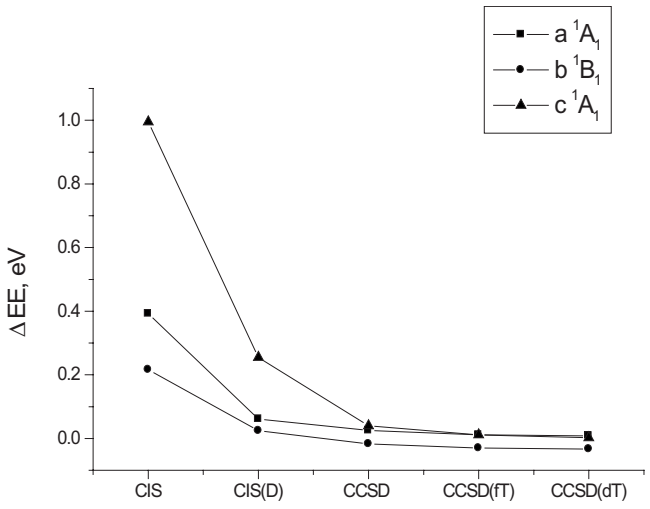

FIG. 2. Differences against SOCI in excitation energies of nitrenium ion, TZ2Pf basis.

TABLE VII. Total energies (hartree) of the ground $X\ ^1A_g$ state of cyclobutadiene and vertical excitation energies (eV) at the $X\ ^1A_g$ equilibrium geometry.

Method	E_{tot} $(X\ ^1A_g)$	$1\ ^3B_{1g}$	$2\ ^1A_{1g}$	$1\ ^1B_{1g}$
EOM-CCSD	−154.416 92	1.346	n/a	3.315
EOM-CCSD(fT)	−154.448 71	1.982	n/a	3.780
EOM-CCSD(dT)	−154.452 52	2.058	n/a	3.814
UHF-EOM-SF-CCSD	−154.424 96	1.654	4.360	3.416
UHF-EOM-SF-CCSD(fT)	−154.429 70	1.516	4.205	3.260
UHF-EOM-SF-CCSD(dT)	−154.429 69	1.475	4.176	3.215
ROHF-EOM-SF-CCSD	−154.425 45	1.656	4.354	3.412
ROHF-EOM-SF-CCSD(fT)	−154.429 76	1.515	4.200	3.256
ROHF-EOM-SF-CCSD(dT)	−154.429 57	1.468	4.170	3.205

At the ground state geometry, where the orbitals are reasonably nondegenerate, we have also performed the EOM-EE calculations. As expected, the magnitude of triples correction is larger for the non-SF wave functions, which describe the multiconfigurational singlet reference state less accurately. The triples correction increases the EOM-EE excitation energies and decreases the SF ones, as seen from Table VII. The absolute values of the (dT) correction for SF are about 0.2 eV for all three excitation energies.

Somewhat unexpectedly, the triples correction increases the discrepancy between the SF and EE excitation energies. We attribute this due to the lack of size intensivity in the EOM-EE variant of the correction. Note that the differences between the EOM states, e.g., the $1\ ^3B_{1g} \rightarrow 1\ ^1B_{1g}$ vertical energy gaps, become closer upon the inclusion of triples, i.e., the EOM-SF-CCSD(fT) and EOM-EE-CCSD(dT) values are within 0.02 eV from each other, whereas the corresponding EOM-CCSD values differ by 0.2 eV.

At the triplet state geometry, the absolute values of the (fT) and (dT) corrections are larger, i.e., (dT) decreases the excitation energies by about 0.3–0.4 eV. The $X\ ^1A_g \rightarrow {}^3A_{2g}$ adiabatic EE as calculated by EOM-SF-CCSD is 0.696 eV. The (fT) and (dT) corrections reduce this value by 0.129 and 0.173 eV, respectively, bringing it down to 0.567 and 0.520 eV.

We also computed adiabatic energy gaps as the differences between the total CCSD, CCSD(fT), and CCSD(dT) energies of the singlet and the high-spin triplet states. The respective values are 0.464, 0.523, and 0.527 eV. These values differ from the above EOM-SF gaps by 0.232, 0.043, and

TABLE VIII. Total energies (hartree) of the ground $X\ ^1B_g$ state of cyclobutadiene and vertical excitation energies (eV) at $1\ ^3A_{2g}$ geometry.

Method	E_{tot} $(X\ ^1B_{1g})$	$1\ ^3A_{2g}$	$2\ ^1A_{1g}$	$1\ ^1B_{2g}$
UHF-EOM-SF-CCSD	−154.413 01	0.369	1.824	2.143
UHF-EOM-SF-CCSD(fT)	−154.414 78	0.163	1.530	1.921
UHF-EOM-SF-CCSD(dT)	−154.413 90	0.098	1.456	1.853
ROHF-EOM-SF-CCSD	−154.413 42	0.369	1.814	2.137
ROHF-EOM-SF-CCSD(fT)	−154.414 77	0.159	1.521	1.915
ROHF-EOM-SF-CCSD(dT)	−154.413 58	0.088	1.438	1.837

TABLE IX. Total energies (hartree) and adiabatic singlet-triplet gaps (eV) in benzynes.

	o-benzyne		*m*-benzyne		*p*-benzyne	
	$^1A_1$	$^3B_2$	$^1A_1$	$^3B_2$	^1A_g	$^3B_{1u}$
SF-CCSD	−230.424 86	1.578	−230.401 62	0.782	−230.380 10	0.147
SF-CCSD(fT)	−230.431 01	1.615	−230.409 53	0.875	−230.385 84	0.169
SF-CCSD(dT)	−230.431 82	1.619	−230.410 76	0.892	−230.386 59	0.172
Expt.[a]		1.628 ± 0.013		0.911 ± 0.014		−0.165 ± 0.016
ΔZPE [b]		−0.028		0.043		0.021
Expt.-ΔZPE		1.656		0.868		0.144

[a]References 76 and 77.
[b]Reference 25.

−0.007 eV, respectively; the improving agreement demonstrating the convergence of the results with respect to the level of correlation treatment.

The UHF and ROHF based results are very similar. At the EOM-CCSD level, the differences in excitation energies are 0.006–0.1 eV, whereas the EOM-SF-CCSD(dT) values differ by 0.010–0.018 eV.

E. *Ortho*-, *meta*-, and *para*-benzynes

The total ground state energies and the adiabatic singlet-triplet gaps in the *ortho*, *meta*, and *para* isomers of the benzyne diradicals are summarized in Table IX.

The singlet and triplet states of the *ortho* and *meta* isomers are of $^1A_1$ and $^3B_2$ symmetry, respectively. The corresponding states for *para*-benzyne are ^1A_g and $^3B_{1u}$.

The absolute values of (dT) correction are 0.025–0.11 eV. The correction increases the singlet-triplet gaps in all the isomers, improving the agreement with the experimental values for the *ortho* and *meta* somers. In *ortho*-benzyne, the triples corrections reduce the error in singlet-triplet gap by half, bringing it down to 0.04 eV. In *meta*-benzyne, SF-CCSD underestimates the gap by 0.086 eV, the (fT) correction slightly overestimates it (by 0.007 eV), and the (dT) correction slightly increases the error to 0.024 eV. In *p*-benzyne, where SF-CCSD is within 0.003 eV from the experimental value, the triples corrections slightly increase the errors up to 0.028 eV. In all three isomers, the SF-CCSD(dT) gaps are within 0.04 eV (0.9 kcal/mol) from the experimental values.

F. 1,2,3 tri-dehydrobenzene

The TDB triradical is a challenging system featuring two nearly degenerate (adiabatically) doublet states,[71] $^2B_2$ and $^2A_1$, derived by distributing three unpaired electrons in the $10a_1$, $7b_2$, and $11a_1$ orbitals.

The results are summarized in Table X. While the vertical energy gaps between the two states are large and are well reproduced by the EOM-SF-CCSD, the adiabatic energy separation is very small, and the adiabatic state ordering is very sensitive to the dynamical correlation.[71]

The triples correction increases the vertical excitation energies by 0.02–0.06 eV. Consistently with the previous results,[71] both SF-CCSD(fT) and SF-CCSD(dT) predict $^2A_1$ to be the ground state, the respective adiabatic energy gaps being 0.03 and 0.05 eV. These values are very close to the CCSD(T) values of 0.07–0.1 eV from Ref. 71.

G. Bond breaking in ethane

The dominant electronic configuration of the ground singlet state of ethane is

$$(\mathrm{core})^2(\sigma_g)^2(\sigma_u^*)^2(\sigma_u)^4(\sigma_g^*)^4(\sigma_g)^2(\sigma_u^*)^0 - \lambda(\mathrm{core})^2(\sigma_g)^2(\sigma_u^*)^2(\sigma_u)^4(\sigma_g^*)^4(\sigma_g)^0(\sigma_u^*)^2. \quad (29)$$

The coefficient λ depends on the bond length—it is small near the equilibrium and increases at stretched geometries, as the wave function acquires multiconfigurational character. The SF method that employs well-behaved $\sigma_g\alpha\sigma_u^*\alpha$ reference is capable of describing this type of bond breaking within a single-reference formalism.

We compare the SF results against the MR-CISD with Davidson's size-extensivity correction (MR-CISD+Q) values from Ref. 63. The data are summarized in Table XI and in Fig. 3. The CCSD absolute errors range between 0.15 and 0.2 eV. The (fT) correction reduces the errors to 0.05–0.1 eV, and the (dT) further reduces it to 0.04–0.09 eV. The nonparallelity errors along the entire curve are 0.049, 0.055, and 0.056 eV for SF-CCSD, SF-CCSD(dT), and SF-CCSD(fT), respectively. Overall, such small differences are comparable with error bars of MR-CISD.

TABLE X. Total energy (hartree) of the $^2B_2$ state and vertical and adiabatic energy differences energies (eV) of the $^2A_1$ state in TDB.

	$^2B_2$	$^2A_1$ [a]	$^2A_1$ [b]	$^2A_1$ [c]
6-31G*				
EOM-SF-CCSD	−229.549 99	1.6355	−4.2112	0.0550
EOM-SF-CCSD(fT)	−229.554 82	1.6420	−4.2453	−0.0284
EOM-SF-CCSD(dT)	−229.555 53	1.6380	−4.2570	−0.0497
cc-pVTZ				
EOM-SF-CCSD	−229.835 01	1.6354	−4.1365	0.0698
EOM-SF-CCSD(fT)	−229.841 88	1.6530	−4.1842	−0.0318
EOM-SF-CCSD(dT)	−229.842 75	1.6526	−4.1955	−0.0502
ROHF-CCSD(T)/cc-VTZ[d]				−0.07
R-CCSD(T)/cc-pVTZ[d]				−0.10
R-CCSD(T)/cc-pVQZ[d]				−0.09

[a]Vertical, at the $^2B_2$ geometry.
[b]Vertical, at the $^2A_1$ geometry.
[c]Adiabatic.
[d]From Ref. 71.

TABLE XI. Total MR-CISD+Q energies (in hartrees) and energy differences (in hartrees) for the SF methods along CC bond-breaking coordinate in ethane.

R_{CC} (Å)	$E^{\text{MR-CISD+}Q}$	$\Delta E^{\text{SF-CCSD}}$	$\Delta E^{\text{SF-CCSD(fT)}}$	$\Delta E^{\text{SF-CCSD(dT)}}$
1.058 36	−79.104 823	−0.238 521	−0.235 468	−0.235 123
1.164 20	−79.301 698	−0.007 356	−0.003 740	−0.003 256
1.270 03	−79.424 633	−0.006 891	−0.003 806	−0.003 446
1.375 87	−79.500 304	−0.006 939	−0.003 729	−0.003 385
1.481 70	−79.545 648	−0.007 017	−0.003 637	−0.003 322
1.587 54	−79.571 362	−0.007 147	−0.003442	−0.003 129
1.693 38	−79.584 366	−0.007 027	−0.002 838	−0.002 505
1.799 21	−79.589 192	−0.006 798	−0.002 285	−0.001 915
1.905 05	−79.588 831	−0.006 633	−0.002 032	−0.001 634
2.010 88	−79.585 276	−0.006 475	−0.001 885	−0.001 475
2.116 72	−79.579 882	−0.006 332	−0.001 811	−0.001 392
2.222 56	−79.573 578	−0.006 208	−0.001 794	−0.001 371
2.328 39	−79.566 996	−0.006 098	−0.001 821	−0.001 398
2.434 23	−79.560 560	−0.006 005	−0.001 884	−0.001 466
2.540 06	−79.554 535	−0.005 923	−0.001 971	−0.001 566
2.645 90	−79.549 077	−0.005 855	−0.002 076	−0.001 689
2.751 74	−79.544 258	−0.005 798	−0.002 190	−0.001 823
2.963 41	−79.536 559	−0.005 711	−0.002 418	−0.002 091
3.175 08	−79.531 179	−0.005 654	−0.002 616	−0.002 325
3.439 67	−79.526 938	−0.005 612	−0.002 802	−0.002 543
3.704 26	−79.524 529	−0.005 590	−0.002 923	−0.002 690
3.968 85	−79.523 199	−0.005 579	−0.002 998	−0.002 782
4.233 44	−79.522 473	−0.005 573	−0.003 041	−0.002 835
4.762 62	−79.521 868	−0.005 568	−0.003 080	−0.002 885
5.291 80	−79.521 692	−0.005 566	−0.003 094	−0.002 904

IV. CONCLUSIONS

We have presented two variants of a noniterative N^7 perturbative triples correction for the EOM-SF/EE-CCSD energies. The corrections are derived using Rayleigh–Schrödiger perturbation theory and employing the CCSD similarity-transformed Hamiltonian as H_0. The two variants of the correction differ by their choice of the TT part of H_0: The (dT) correction uses the diagonal elements of $\bar{H}$, whereas the (fT) correction employs Hartree–Fock orbital energy differences. The former correction is not orbital invariant, whereas the latter is. Numerically, the (dT) correction demonstrates slightly better performance.

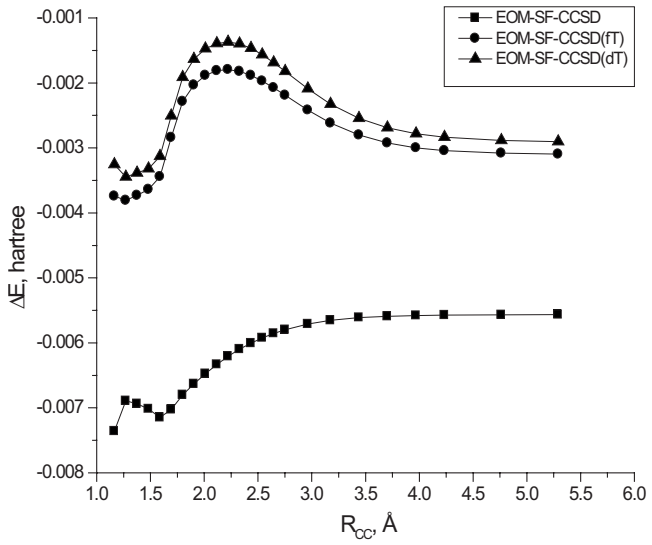

FIG. 3. Energy differences against MR-CISD+Q along the CC bond-breaking coordinate in ethane, aug-cc-pVTZ.

The SF variant of the corrections is size intensive. The performance of the correction is demonstrated by the numerical examples, e.g., methylene, nitrenium ion, cyclobutadiene, *ortho*-, *meta*-, and *para*-benzynes, TDB, as well as C–C bond breaking in ethane. For selected systems, we compare the SF and EE variants of the correction. In all cases except cyclobutadiene, the absolute values of the correction for energy differences were 0.1 eV or less. In cyclobutadiene, the absolute value of the correction was as large as 0.4 eV, which slightly exceeds the conservative estimate of EOM-CCSD error bars. In most cases, the corrections reduced the errors against the benchmark values by a factor of 2–3, the absolute errors being less than 0.04 eV.

ACKNOWLEDGMENTS

This work was conducted under the auspices of the *iOpenShell* Center for Computational Studies of Electronic Structure and Spectroscopy of Open-Shell and Electronically Excited Species (iopenshell.usc.edu) supported by the National Science Foundation through the CRIF:CRF Grant Nos. CHE-0625419, 0624602, and 0625237. A.I.K. also gratefully acknowledges support of the National Science Foundation through the Grant No. CHE-0616271. We would like to thank Professor John Stanton for insightful comments and a critical feedback on the manuscript and to Professor Piotr Piecuch for helpful discussions and help in deriving programmable expressions for the CR-CCSD(T)$_L$ method.

APPENDIX: IMPLEMENTATION

As follows from Eq. (21), the calculation of the noniterative energy correction involves contraction of three six-index tensors, $\tilde{\sigma}$, σ, and D^m. Explicit calculation of these tensors leads to N^6 disk requirements. Therefore, the efficient implementation should avoid explicit calculation of the six-index quantities and directly compute the respective contributions to the energy. To make an efficient use of our block-tensor library,[73,74] which was designed to handle large tensors and incorporates spatial and spin symmetry, we break down the tensors into smaller arrays of reduced dimensionality tensors by the so-called unrolling. For example, instead of generating six-index block tensor σ_{ijkabc}, one can form an ijk array of abc block tensors. We use upper case letters to denote the unrolled indexes, e.g., $\sigma_{abc}(IJK)$, $\tilde{\sigma}_{abc}(IJK)$, and $D^m_{abc}(IJK)$ represent the IJK-unrolled σ^{abc}_{ijk}, $\tilde{\sigma}^{abc}_{ijk}$, and D^m_{ijkabc} tensors from Eq. (21). In these notations, the energy correction assumes the following form:

$$E^{(2)}_m = -\frac{1}{(3!)^2}\sum_{IJK}\sum_{abc}\frac{\tilde{\sigma}_{abc}(IJK)\sigma_{abc}(IJK)}{D^m_{abc}(IJK)} \tag{A1}$$

and is calculated as follows: For each IJK, the reduced dimensionality block tensors $\sigma_{abc}(IJK)$, $\tilde{\sigma}_{abc}(IJK)$, and $D^m_{abc}(IJK)$ are computed, contracted as specified by Eq. (A1), and discarded. This implementation takes full advantage of spatial and spin symmetry.

The $\tilde{\sigma}$ vectors from Eq. (A1) are

$$\tilde{\sigma}_{abc}(I,J,K) = \langle \Phi_0 L_1 | \bar{H} | \Phi_{IJK}^{abc} \rangle + \langle \Phi_0 L_2 | \bar{H} | \Phi_{IJK}^{abc} \rangle, \tag{A2}$$

where

$$\langle \Phi_0 L_1 | \bar{H} | \Phi_{IJK}^{abc} \rangle = P(a|bc)(l_I^a \langle JK||bc\rangle - l_J^a \langle IK||bc\rangle + l_K^a \langle IJ||bc\rangle), \tag{A3}$$

$$\begin{aligned}\langle \Phi_0 L_2 | \bar{H} | \Phi_{IJK}^{abc} \rangle = {} & P(a|bc)(l_{JK}^{bc} F_{Ia} - l_{IK}^{bc} F_{Ja} + l_{IJ}^{bc} F_{Ka}) \\ & - P(ab|c) \sum_l (l_{Il}^{ab} I_{JKlc}^6 - l_{Jl}^{ab} I_{IKlc}^6 + l_{Kl}^{ab} I_{IJlc}^6) \\ & + P(a|bc) \sum_d (l_{IJ}^{ad} I_{Kdcb}^7 - l_{IK}^{ad} I_{Jdcb}^7 \\ & + l_{JK}^{ad} I_{Idcb}^7).\end{aligned} \tag{A4}$$

Thus, the calculation of the above terms requires the following unrolled integrals and intermediates: l_I^a, l_{JK}^{bc}, l_{Il}^{ab}, $\langle JK||bc\rangle$, I_{JKlc}^6, and I_{Kdcb}^7, which are obtained from the corresponding intermediates[5,59,60] by unrolling. The equations for $\sigma_{abc}(IJK)$ are easily derived in a similar fashion.

The diagonal is calculated in a slightly different manner. The diagonal expression can be divided into *IJK*, *abc*, and *IJKabc* parts. The *IJK* term is just a number and is computed inside the *IJK* loop. The *abc* part is calculated once and is then used whenever required. The part depending on both *IJK* and *abc* is generated for every *IJK*, similarly to calculation of $\tilde{\sigma}_{abc}(IJK)$ described above. The diagonal can thus be written as

$$D_{abc}^m(IJK) = (Dijk(IJK) - \omega_m) + Dabc^{abc} + \tilde{D}_{abc}(IJK), \tag{A5}$$

where

$$Dijk(IJK) = -F_{II} - F_{JJ} - F_{KK} + 2I_{IJIJ}^4 + 2I_{IKIK}^4 + 2I_{JKJK}^4, \tag{A6}$$

$$Dabc^{abc} = P(abc)F_{aa} + 2 \cdot P(ab|c)I_{abab}^5,$$

$$\begin{aligned}\tilde{D}_{abc}(IJK) = {} & -P(abc)(I_{IaIa}^1 + I_{JaJa}^1 + I_{KaKa}^1) \\ & - P(abc) \sum_d (t_{IJ}^{ad} \langle IJ||ad\rangle + t_{IK}^{ad} \langle IK||ad\rangle \\ & + t_{JK}^{ad} \langle JK||ad\rangle) - P(abc) \sum_l (t_{Il}^{ab} \langle Il||ab\rangle \\ & + t_{Jl}^{ab} \langle Jl||ab\rangle + t_{Kl}^{ab} \langle Kl||ab\rangle).\end{aligned} \tag{A7}$$

[1] D. J. Rowe, Rev. Mod. Phys. **40**, 153 (1968).
[2] K. Emrich, Nucl. Phys. A **351**, 379 (1981).
[3] J. Geertsen, M. Rittby, and R. J. Bartlett, Chem. Phys. Lett. **164**, 57 (1989).
[4] J. F. Stanton and R. J. Bartlett, J. Chem. Phys. **98**, 7029 (1993).
[5] S. V. Levchenko and A. I. Krylov, J. Chem. Phys. **120**, 175 (2004).
[6] D. Sinha, D. Mukhopadhyay, and D. Mukherjee, Chem. Phys. Lett. **129**, 369 (1986).
[7] S. Pal, M. Rittby, R. J. Bartlett, D. Sinha, and D. Mukherjee, Chem. Phys. Lett. **137**, 273 (1987).
[8] J. F. Stanton and J. Gauss, J. Chem. Phys. **101**, 8938 (1994).
[9] M. Nooijen and R. J. Bartlett, J. Chem. Phys. **102**, 3629 (1995).
[10] D. Mukherjee and S. Pal, Adv. Quantum Chem. **20**, 291 (1989).
[11] R. J. Bartlett and J. F. Stanton, Rev. Comput. Chem. **5**, 65 (1994).
[12] R. J. Bartlett, Int. J. Mol. Sci. **3**, 579 (2002).
[13] J. F. Stanton and J. Gauss, Adv. Chem. Phys. **125**, 101 (2003).
[14] A. I. Krylov, Acc. Chem. Res. **39**, 83 (2006).
[15] O. Christiansen, Theor. Chim. Acta **116**, 106 (2006).
[16] A. I. Krylov, Annu. Rev. Phys. Chem. **59**, 433 (2008).
[17] H. J. Monkhorst, Int. J. Quantum Chem., Quantum Chem. Symp. **11**, 421 (1977).
[18] H. Sekino and R. J. Bartlett, Int. J. Quantum Chem., Quantum Chem. Symp. **26**, 255 (1984).
[19] H. Koch, H. J. Aa Jensen, P. Jørgensen, and T. Helgaker, J. Chem. Phys. **93**, 3345 (1990).
[20] M. Head-Gordon and T. J. Lee, in *Modern Ideas in Coupled Cluster Theory*, edited by R. J. Bartlett (World Scientific, Singapore, 1997).
[21] H. Nakatsuji and K. Hirao, J. Chem. Phys. **68**, 2053 (1978).
[22] H. Nakatsuji, Chem. Phys. Lett. **177**, 331 (1991).
[23] H. Koch and P. Jørgensen, J. Chem. Phys. **93**, 3333 (1990).
[24] H. Larsen, K. Hald, J. Olsen, and P. Jørgensen, J. Chem. Phys. **115**, 3015 (2001).
[25] L. V. Slipchenko and A. I. Krylov, J. Chem. Phys. **117**, 4694 (2002).
[26] S. Hirata, M. Nooijen, and R. J. Bartlett, Chem. Phys. Lett. **326**, 255 (2000).
[27] L. V. Slipchenko and A. I. Krylov, J. Chem. Phys. **123**, 084107 (2005).
[28] M. Kállay and J. Gauss, J. Chem. Phys. **121**, 9257 (2004).
[29] K. W. Sattelmeyer, J. F. Stanton, J. Olsen, and J. Gauss, Chem. Phys. Lett. **347**, 499 (2001).
[30] S. A. Kucharski, M. Włoch, M. Musiał, and R. J. Bartlett, J. Chem. Phys. **115**, 8263 (2001).
[31] K. Kowalski and P. Piecuch, J. Chem. Phys. **115**, 643 (2001).
[32] M. Kállay and P. R. Surjan, J. Chem. Phys. **113**, 1359 (2000).
[33] S. Hirata, J. Chem. Phys. **121**, 51 (2004).
[34] J. D. Watts and R. J. Bartlett, J. Chem. Phys. **101**, 3073 (1994).
[35] J. Noga, R. J. Bartlett, and M. Urban, Chem. Phys. Lett. **134**, 126 (1987).
[36] J. D. Watts and R. J. Bartlett, Chem. Phys. Lett. **233**, 81 (1995).
[37] J. D. Watts and R. J. Bartlett, Chem. Phys. Lett. **258**, 581 (1996).
[38] H. Koch, O. Christiansen, P. Jørgensen, and J. Olsen, Chem. Phys. Lett. **244**, 75 (1995).
[39] O. Christiansen, H. Koch, and P. Jorgensen, J. Chem. Phys. **103**, 7429 (1995).
[40] O. Christiansen, H. Koch, and P. Jorgensen, J. Chem. Phys. **105**, 1451 (1996).
[41] C. E. Smith, R. A. King, and T. D. Crawford, J. Chem. Phys. **122**, 054110 (2005).
[42] K. Kowalski and P. Piecuch, J. Chem. Phys. **113**, 18 (2000).
[43] K. Kowalski and P. Piecuch, J. Chem. Phys. **115**, 2966 (2001).
[44] K. Kowalski and P. Piecuch, J. Chem. Phys. **120**, 1715 (2004).
[45] P. Piecuch, M. Włoch, J. R. Gour, and A. Kinal, Chem. Phys. Lett. **418**, 463 (2005).
[46] P. Piecuch and M. Włoch, J. Chem. Phys. **123**, 224105 (2005).
[47] M. Włoch, M. D. Lodriguito, P. Piecuch, and J. R. Gour, Mol. Phys. **104**, 2149 (2006).
[48] T. D. Crawford and J. F. Stanton, Int. J. Quantum Chem. **70**, 601 (1998).
[49] S. A. Kucharski and R. J. Bartlett, J. Chem. Phys. **108**, 5243 (1998).
[50] S. R. Gwaltney, C. D. Sherrill, M. Head-Gordon, and A. I. Krylov, J. Chem. Phys. **113**, 3548 (2000).
[51] S. R. Gwaltney and M. Head-Gordon, J. Chem. Phys. **115**, 2014 (2001).
[52] A. G. Taube and R. J. Bartlett, J. Chem. Phys. **128**, 044110 (2008).
[53] A. G. Taube and R. J. Bartlett, J. Chem. Phys. **128**, 044111 (2008).
[54] K. Raghavachari, G. W. Trucks, J. A. Pople, and M. Head-Gordon, Chem. Phys. Lett. **157**, 479 (1989).
[55] J. D. Watts, J. F. Stanton, and R. J. Bartlett, Chem. Phys. Lett. **178**, 471 (1991).
[56] J. F. Stanton and J. Gauss, Theor. Chim. Acta **93**, 303 (1996).
[57] S. Hirata, M. Nooijen, I. Grabowski, and R. J. Bartlett, J. Chem. Phys. **114**, 3919 (2001).
[58] J. D. Watts, S. R. Gwaltney, and R. J. Bartlett, J. Chem. Phys. **105**, 6979 (1996).
[59] A. I. Krylov, C. D. Sherrill, and M. Head-Gordon, J. Chem. Phys. **113**, 6509 (2000).
[60] S. V. Levchenko, T. Wang, and A. I. Krylov, J. Chem. Phys. **122**, 224106 (2005).
[61] Size extensivity of EOM-CC often causes confusion. For the two noninteracting fragments A and B, there are three different types of the EOM

target states: (i) The EOM excited states of A and B being in the ground state; (ii) the EOM states of B and A is in the ground state; and (iii) simultaneous excitations on A and B. Whereas the EOM excitation energies of states (i) and (ii) are exactly the same as the EOM excitation energies of the individual fragments, the excitation energies of (iii) are not the sum of the corresponding excitation energies of A and B. Thus, only the energies of states from (i) and (ii) are size extensive, provided that the reference wave function is size extensive as well. For example, the EOM-EE-CCSD total energies of the lowest excited states of Be and Ne, which are 100 Å apart, are equal to the EOM total energies of the corresponding Be state plus the CCSD energy of Ne. However, excitation energies of the states in which both Be and Ne are excited (i.e., doubly excited states of the combined system) are not the sum of the respective EOM-EE energies of the monomers and are, therefore, not size extensive. Thus, size extensivity of EOM is weaker than that of CC (e.g., the total CCSD energy of Be–Ne is the sum of the CCSD energies of the atoms), but stronger that that of the truncated CI (e.g., CISD excited states of Be are affected by the Ne atom 100 Å away). To emphasize this difference, the term size intensivity is commonly employed. The important point is that the quality of the EOM treatment does not degrade with the molecular size, provided that the excited states are localized on chromophore groups, as, for example, in the $CH_2O \rightarrow CH_3CHO \rightarrow CH_3(CH_2)_nCHO$ series. Moreover, EOM-EE describes well those electronic states of bichromophores (or polychromophers), which are linear combinations of single excitations of the chromophores, e.g., excimer states in the benzene dimer or ionized states in the benzene dimer cation. See also discussion in Ref. 16.

[62] Y. Shao, L. F. Molnar, Y. Jung, J. Kussmann, C. Ochsenfeld, S. Brown, A. T. B. Gilbert, L. V. Slipchenko, S. V. Levchenko, D. P. O'Neil, R. A. Distasio, Jr., R. C. Lochan, T. Wang, G. J. O. Beran, N. A. Besley, J. M. Herbert, C. Y. Lin, T. Van Voorhis, S. H. Chien, A. Sodt, R. P. Steele, V. A. Rassolov, P. Maslen, P. P. Korambath, R. D. Adamson, B. Austin, J. Baker, E. F. C. Bird, H. Daschel, R. J. Doerksen, A. Drew, B. D. Dunietz, A. D. Dutoi, T. R. Furlani, S. R. Gwaltney, A. Heyden, S. Hirata, C.-P. Hsu, G. S. Kedziora, R. Z. Khalliulin, P. Klunziger, A. M. Lee, W. Z. Liang, I. Lotan, N. Nair, B. Peters, E. I. Proynov, P. A. Pieniazek, Y. M. Rhee, J. Ritchie, E. Rosta, C. D. Sherrill, A. C. Simmonett, J. E. Subotnik, H. L. Woodcock III, W. Zhang, A. T. Bell, A. K. Chakraborty, D. M. Chipman, F. J. Keil, A. Warshel, W. J. Herhe, H. F. Schaefer III, J. Kong, A. I. Krylov, P. M. W. Gill, and M. Head-Gordon, Phys. Chem. Chem. Phys. **8**, 3172 (2006).

[63] A. Golubeva, A. V. Nemukhin, L. Harding, S. J. Klippenstein, and A. I. Krylov, J. Phys. Chem. A **111**, 13264 (2007).

[64] C. D. Sherrill, M. L. Leininger, T. J. Van Huis, and H. F. Schaefer III, J. Chem. Phys. **108**, 1040 (1998).

[65] J. C. Stefens, Y. Yamaguchi, C. D. Sherrill, and H. F. Schaefer III, J. Phys. Chem. **102**, 3999 (1998).

[66] S. Huzinaga, J. Chem. Phys. **42**, 1293 (1965).

[67] T. H. Dunning, J. Chem. Phys. **55**, 716 (1971).

[68] T. H. Dunning, J. Chem. Phys. **90**, 1007 (1989).

[69] A. I. Krylov, Chem. Phys. Lett. **338**, 375 (2001).

[70] Y. Shao, M. Head-Gordon, and A. I. Krylov, J. Chem. Phys. **118**, 4807 (2003).

[71] L. Koziol, M. Winkler, K. N. Houk, S. Venkataramani, W. Sander, and A. I. Krylov, J. Phys. Chem. A **111**, 5071 (2007).

[72] See EPAPS Document No. E-JCPSA6-129-001843 for the molecular structures and total energies. For more information on EPAPS, see http://www.aip.org/pubservs/epaps.html.

[73] A. I. Krylov, C. D. Sherrill, and M. Head-Gordon (unpublished).

[74] T. L. Windus and J. A. Pople, Int. J. Quantum Chem. **56**, 485 (1995).

[75] S. Gibson, J. Greene, and J. Berkowitz, J. Chem. Phys. **83**, 4319 (1985).

[76] P. G. Wenthold, J. Hu, and R. R. Squires, J. Am. Chem. Soc. **118**, 11865 (1996).

[77] P. G. Wenthold, R. R. Squires, and W. C. Lineberger, J. Am. Chem. Soc. **120**, 5279 (1998).